



Mechanisms for reactions of trimethylaluminum with molecular oxygen and water



Hue M.T. Nguyen^{a,*}, Hsin-Yu Tang^b, Wen-Fei Huang^b, M.C. Lin^{b,*}

^a Faculty of Chemistry and Center for Computational Science, Hanoi National University of Education, Viet Nam

^b Center for Interdisciplinary Molecular Science, Department of Applied Chemistry, National Chiao Tung University, Hsinchu 300, Taiwan

ARTICLE INFO

Article history:

Received 14 February 2014

Accepted 14 February 2014

Available online 3 March 2014

Keywords:

Reaction mechanism

(CH₃)₃Al (TMA)

O₂

H₂O and dimethylaluminum (DMA) DFT

(B3LYP)

(U)CCSD(T)

Potential energy surface

ABSTRACT

(CH₃)₃Al (TMA) has been employed for preparation of various thin films. It is also known to be hypergolic in the air. To unveil the hypergolic phenomenon, the mechanism for the reaction of TMA with O₂ and/or H₂O molecules is studied using computational quantum methods. Our results show that TMA reacts with water much faster than with O₂, and water is not an efficient catalyst to help O₂ reacting with TMA. The reactions of TMA with water and oxygen molecules can undergo subsequent ones in the air. However, the barrier predicted for production of CH₃ was found to be too high for combustion initiation under the ambient condition.

© 2014 Elsevier B.V. All rights reserved.

1. Introduction

The group III–VI materials have been the subject of significant interest, in part due to the fact that they are wide-gap semiconductor materials for potential photovoltaic or optoelectronic applications [1–5]. Trimethylaluminum (TMA) is well known as an aluminum source used in semiconductor fabrication to grow thin films, such as Al₂O₃ and aluminum nitride (AlN) via different processes of atomic layer deposition (ALD) or metal organic chemical vapor deposition (MOCVD) [6–11]. The role of Al₂O₃ thin films is important as insulator and passivating layers in many different applications and it was the first dielectric oxide deposited by ALD, though the precursors in that process are AlCl₃ and water [12]. The reason for using TMA to fabricate Al₂O₃ thin films is that trimethylaluminum is a thermally stable high vapor pressure (8.4 Torr) liquid at room temperature and easily reacts with water to produce Al₂O₃. The interesting features of aluminum nitride (AlN) include a range of unique physical properties from a large band gap (6.2 eV) and high electrical resistivity, to low dielectric loss and high thermal conductivity [13]. Consequently, thin films of AlN have a wide range of applications in electronics, such as insulating layers in metal–insulator–semiconductor devices [14],

in microelectronics packaging [15] and in surface-acoustic wave devices for chemical sensors [16]. In fabricating a light emitting element using this nitride semiconductor, growing a crystal of a nitride semiconductor thin film by a metal–organic chemical vapor deposition (MOCVD) method is the mainstream. This technique is thus carried out, and in fact trimethylaluminum (TMA) is one of effective compounds to produce aluminum nitride thin films, due to the fact that it could be deposited from the reaction between TMA and ammonia [17]. Beside the part of supplying aluminum source to fabricate thin film, trimethylaluminum is also known as one of the industrially important organometallic compounds [18]. It is used to play the role of co-catalyst for polymerization of alkenes in conjunction with homogeneous Ziegler–Natta catalysts such as halides of titanium or vanadium [19]. Research work over the last decades showed that alkylaluminums are also active as co-catalysts along with aluminoxanes in polymerization reactions catalyzed by metallocenes [20,21].

Another application of trimethylaluminum is that it can be used as an ignitor for jet and rocket engines. In this regard, TMA has been considered as a pyrophoric colorless liquid compound. In fact this liquid spontaneously bursts into flames if exposed to air, and reacts explosively with water. Thus, an atmosphere of dry nitrogen or argon is required for handling and storage of TMA. In this context, a major goal of the present research is about how it happens when it is in contact with the air containing a considerable amount of oxygen and water. To understand the underlying mechanisms,

* Corresponding authors. Tel.: +84 438330842 (H.M.T. Nguyen).

E-mail addresses: hue.nguyen@hnue.edu.vn (H.M.T. Nguyen), chemmcl@emory.edu (M.C. Lin).

our strategy for the present work is to search for elementary reactions in which a large amount of energy is released, together with reactive radical products such as CH_3 are generated to initiate a chain process. The reactions investigated include $(\text{CH}_3)_3\text{Al} + \text{O}_2$, $(\text{CH}_3)_3\text{Al} + \text{H}_2\text{O}$ and $(\text{CH}_3)_3\text{Al} + \text{H}_2\text{O} + \text{O}_2$. Beside these reactions, we have also considered another important reaction between dimethylaluminum (DMA) with water, because DMA is one of the intermediate decomposition products formed from these processes. The results of this work are presented herein.

2. Quantum chemical methods

All electronic structure calculations were performed using the Gaussian 03 suite of programs [22]. Geometrical parameters of the structures considered were initially optimized using the MO methods at the Hartree–Fock (HF) level and the stationary points were subsequently characterized by harmonic vibrational analyses. Geometries of the relevant equilibrium structures and transition structures were then re-optimized using the density functional theory (DFT) with the popular hybrid B3LYP functional in conjunction with the polarized plus diffuse functions 6-311++G(3df,2p) basis set. The zero-point energy (ZPE) corrections to the relative energies were also obtained at the latter level, but applying a scaling factor of 0.97. The unrestricted formalism is used for open shell systems (UHF, UB3LYP...). In order to further improve the relative energies between stationary structures, single-point electronic energy calculations were finally computed using the coupled-cluster theory, incorporating all the single and double excitations plus perturbative corrections for the triple excitations, (U)CCSD(T) with the 6-311+G(d,p) and 6-311+G(3df,2p). Spin contamination was not high as was judged by the expectation values of S^2 .

3. Results and discussion

3.1. Reactions of trimethylaluminum $(\text{CH}_3)_3\text{Al}$ with O_2

Trimethylaluminum (TMA) is formed when one Al atom binds three methyl groups. As each of these bonds contains a pair of electrons, then it is surrounded by six electrons. TMA has a planar structure but with small rotational energy barriers of the methyl groups. This implies that one Al 3s and two Al 3p orbitals hybridize to form three sp^2 orbitals bonding with $-\text{CH}_3$ ligands, and an empty p orbital is left on the Al atom [23]. The C–Al bond length is 1.965 Å (move up from the next section). Although the carbon atoms of the methyls are surrounded each by four neighbors, they have eight electrons in their outer shells. This electron-deficiency causes TMA to be very reactive with respect to any substance that may offer electrons. It readily undergoes exchanges of methyls for others groups and/or atoms bearing more electrons. This property makes TMA an excellent methylation agent.

$(\text{CH}_3)_2\text{AlO}_2$ is a potential product of the addition of TMA with molecular oxygen. From its doublet state, the CH_3 radical is generated, which in turns may initiate a chain reaction in the air. A transition structure and an intermediate formed from this process are both in the triplet state. The detail of the release of CH_3 is described in Fig. 1.

Portions of the potential energy surface (PES) corresponding the reaction of the singlet TMA and the triplet O_2 is displayed in Fig. 1, along with the selected parameters of the optimized geometries of the reactants, transition structures, intermediates and products obtained at the CCSD(T)/6-311+G(3df,2p)//B3LYP/6-311++G(3df,2p) level. The $(\text{CH}_3)_3\text{AlO}_2$ intermediate is formed by attachment of both atoms of the molecular oxygen, simultaneously bound to a TMA aluminum center through TS_{1a} , giving rise to a bridged adduct. This

transition structure is about 16.9 kcal/mol higher in energy than the reactants (values at CCSD(T)/6-311+G(3df,2p) + ZPE). The intermediate and product $(\text{CH}_3)_2\text{AlO}_2 + \text{CH}_3$ are also predicted to be slightly higher in energy than the reactants, by 5.8 and 8.2 kcal/mol, respectively.

The predicted geometries provide useful information on the reaction mechanism. The O–O bond and one of the Al–C bonds are elongated by 0.084 Å and 0.154 Å in going from the reactants and the transition state. The two Al...O distances are calculated to be about 2.0 and 2.176 Å in the TS_{1a} structure. The bond length changes in Al–C, O–O and Al–O, suggest that this step is clearly defined as the critical motions of the transition state. The $(\text{CH}_3)_3\text{AlO}_2$ intermediate obtained is a three-membered ring triplet compound, in which the O–O and two Al–C bond lengths are 1.344, 1.925 and 1.958 Å, respectively. This indicates that an Al–C bond is much weaker than the other two Al–C counterparts. The distance is estimated at ~ 2.611 Å. To form the final products, namely $(\text{CH}_3)_2\text{AlO}_2 + \text{CH}_3$, one of the CH_3 groups needs to be ejected from $(\text{CH}_3)_3\text{AlO}_2$, and in fact, the CH_3 group is expelled from the most elongated Al–C bond. As seen in the PES, this Al–C bond is very weak, and it is broken to form the free methyl radical product by a small dissociation energy of ~ 2.4 kcal/mol. No transition structure has been found for this simple bond cleavage. In the final product, the Al–C bond length is shortened to 1.947 Å in $(\text{CH}_3)_2\text{AlO}_2$, and the Al–O distance is also decreased to 1.890 Å. In this regard, the Al–O bond is stronger in $(\text{CH}_3)_2\text{AlO}_2$ than in $(\text{CH}_3)_3\text{AlO}_2$, as one would expect. The O–O bond length is now increased to 1.348 Å in the $(\text{CH}_3)_2\text{AlO}_2$ product.

In summary, the reaction between TMA and O_2 is characterized by a barrier height of 16.9 kcal/mol, which is the rate-determining step (Fig. 1). The intermediate is not stable giving rise to the final products $(\text{CH}_3)_2\text{AlO}_2 + \text{CH}_3$ by simple bond cleavage. After these products are formed, then they can lead to subsequent reactions in the air.

3.2. Reactions of trimethylaluminum $(\text{CH}_3)_3\text{Al}$ with H_2O

Similar to the $(\text{CH}_3)_3\text{Al} + \text{O}_2$ reaction, we explore in detail the mechanism for the reaction of $(\text{CH}_3)_3\text{Al} + \text{H}_2\text{O}$ using two different methods B3LYP and CCSD(T). All the geometries were optimized at the B3LYP/6-311++G(3df,2p) level, and in order to further improve the relative energies between stationary structures, single-point energy calculations were subsequently computed at the CCSD(T)/6-311+G(3df,2p) level and corrected for ZPEs. Profile of the potential energy illustrating the reaction, and selected optimized geometries are shown in Fig. 2.

Starting from the reactants $\text{Al}(\text{CH}_3)_3 + \text{H}_2\text{O}$, the empty p orbital of TMA can interact with the incoming H_2O lone pair electron [23] to form a stable adduct $(\text{CH}_3)_3\text{Al}:\text{OH}_2$ (Fig. 2). This intermediate is easily formed by a strong interaction between strong Al and O atoms. The Al–O bond length is 2.092 Å, which is close to the Al–O distance when TMA bonding with an $-\text{OH}$ ligand on the silicon surface [24]. Another reason for making this compound more stable is that the two reactants holds together by an $\text{OH}\cdots\text{C}$ hydrogen bond. In fact, the binding energy is the sum of two contributions, and it amounts to -15.1 kcal/mol.

Decomposition of the $(\text{CH}_3)_3\text{Al}:\text{OH}_2$ adduct may produce CH_4 and a stable molecule, $(\text{CH}_3)_2\text{AlOH}$. The TS_{1b} is formed by one of the two H atoms of water interacting with one of the CH_3 ligands in this process. The values of two O–Al–C and HOAl angles decrease by large amounts (17 – 45°) and the Al–O bond length decreases from 2.092 to 1.909 Å, while Al–C bond length increases from 1.984 to 2.156 Å. The transition vector is dominated by the migration of hydrogen, which is 1.181 Å away from the O atom and 1.5 Å in its interaction with the C atom. The energy barrier via TS_{1b} is calculated at ~ 15 kcal/mol above the complex. Formation of

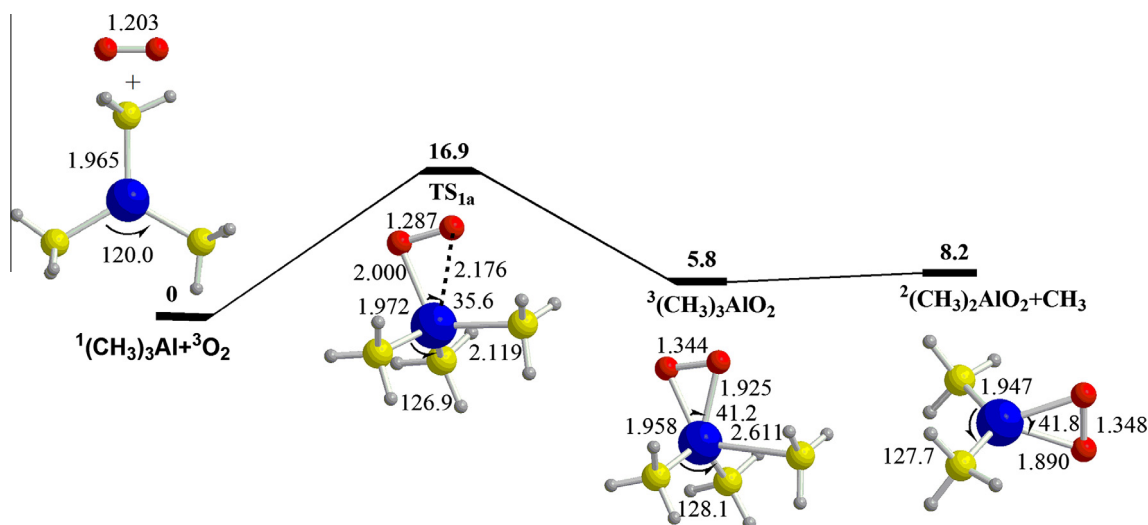


Fig. 1. Potential energy profile showing the $(\text{CH}_3)_3\text{Al} + \text{O}_2$ reaction. Relative energies (kcal/mol) are calculated using the CCSD(T)/6-311+G(3df,2p)//B3LYP/6-311+G(3df,2p) + ZPE level. Selected bond lengths are given in angstrom and angles in degree.

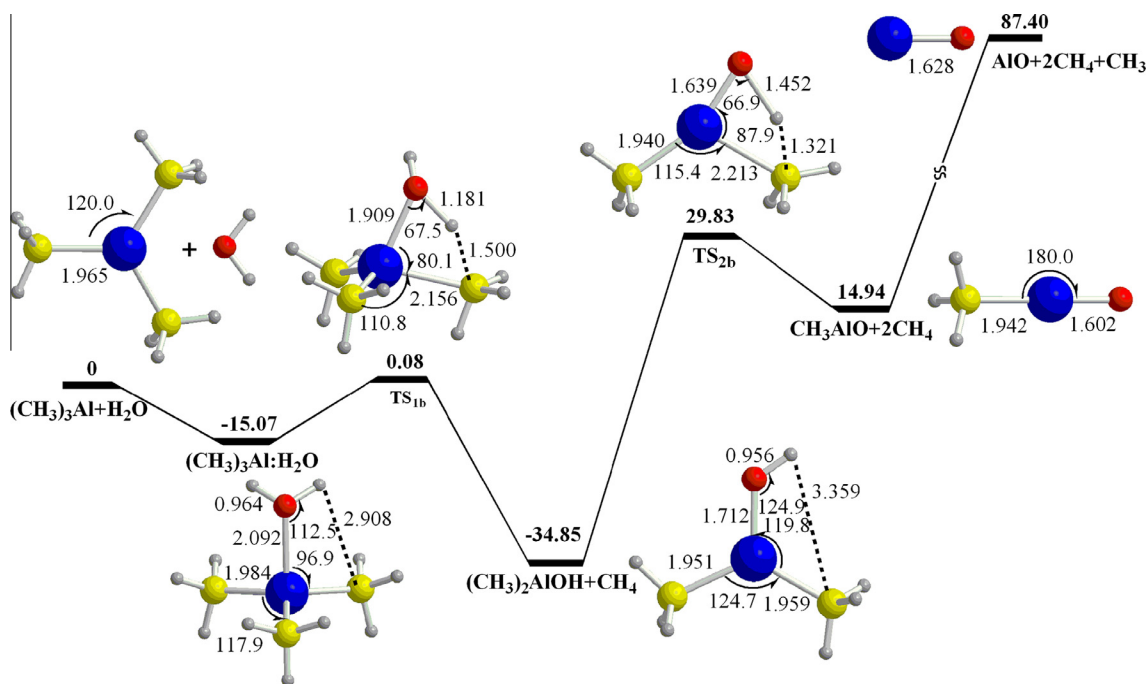


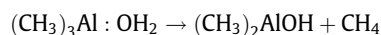
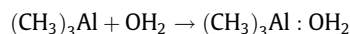
Fig. 2. Potential energy profile showing the $(\text{CH}_3)_3\text{Al} + \text{H}_2\text{O}$ reaction. Relative energies (kcal/mol) are calculated using the CCSD(T)/6-311+G(3df,2p)//B3LYP/6-311+G(3df,2p) + ZPE level. Selected bond lengths are given in angstrom and angles in degree.

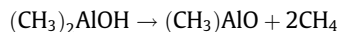
$(\text{CH}_3)_2\text{AlOH} + \text{CH}_4$ is found to be exothermic by -34.9 kcal/mol at the CCSD(T)/B3LYP level.

The $(\text{CH}_3)_2\text{AlOH}$ molecule can further rearrange to give another CH_4 and CH_3AlO (as seen in Fig. 2), with a rather large energy barrier (29.8 kcal/mol) via TS_{2b} . The O–Al–C angle at TS_{2b} decreases from 119.8° in $(\text{CH}_3)_2\text{AlOH}$ to 87.9° in TS_{2b} . This also suggests that the transition vector is dependent on the motion of hydrogen and it is similar to TS_{1b} . We should notice that the distance from H to O is 1.452 Å and from H to C is 1.321 Å. The Al–C bond length is elongated from 1.959 to 2.213 Å, which is a significant variation. TS_{2b} leads to CH_3AlO and CH_4 can release ~ 15 kcal/mol. The endothermic heat of reaction forming $\text{CH}_3\text{AlO} + 2\text{CH}_4$ products is predicted to be 14.9 kcal/mol. CH_3AlO has a C_{3v} point group with the linear AlO framework. The bond lengths of Al–O and Al–C are 1.602

and 1.942 Å, respectively. Furthermore, the decomposition of CH_3AlO by bond cleavage giving two doublet radicals, $\text{CH}_3 + \text{AlO}$, and the dissociation energy is 87.4 kcal/mol. The doublet electronic ground state of AlO has a bond length of 1.628 Å, which is longer than that in CH_3AlO (1.602 Å). In the potential energy surface shown in Fig. 2, the dissociation energy for the final products is 87.4 kcal/mol higher energy than the reactants by CCSD(T)//B3LYP calculations.

The overall reaction mechanisms for the interaction between trimethylaluminum with H_2O can be written as follows:





In these reactions, the first two reactions are exothermic and can readily occur, whereas the last two processes are endothermic and thus more difficult to achieve. The barrier to formation of CH_3AlO is 29.8 kcal/mol, which is not easily overcome at the ambient temperature.

3.3. Reactions of trimethylaluminum $(\text{CH}_3)_3\text{Al}$ with H_2O and O_2

The geometries of the reactants, intermediates, transition states and products in this reaction were optimized by B3LYP/6-311++G(3df,2p), but due to the fact that the number of heavy atoms increases in this system, then we calculated single point electronic energies by using a smaller basis set, namely at the CCSD(T)/6-311+G(d,p) level. Profile of the potential energy illustrating the reaction, and selected optimized geometries are shown in Fig. 3. In this process, we consider a water molecule as a catalyst to help the O_2 molecule to interact with TMA. Firstly, water binds to TMA with an exothermicity of ~ 15.7 kcal/mol. The geometries of both the TMA and H_2O are not much changed when the complex is formed. All the Al–C bond lengths remain similar (from 1.965 to 1.985 Å). The O–H bond remains unchanged upon formation of $(\text{CH}_3)_3\text{Al}:\text{OH}_2$. The C–Al–C bond angle marginally decreases from 120.0 to 117.9°. The TMA– OH_2 adduct is stable comparing with the reactants, and it continues to react with O_2 leading to formation of TMA– $\text{OH}_2:\text{O}_2$. The energy release for this process is ~ 1.3 kcal/mol. In fact, the TMAI– OH_2 molecule binds to O_2 essentially by hydrogen bond. This interaction is weak and the geometry of TMAI– $\text{OH}_2:\text{O}_2$ complex does not change with respect to the fragments. From this complex, $(\text{CH}_3)_2\text{Al}(\text{O}_2)\text{OH}_2$ and one CH_3 radical are formed via the transition structure TS_{1d} with a relative energy of 19.4 kcal/mol. The Al–O bond is formed upon a significant decrease from 2.216 (TS_{1d}) to 1.909 Å ($(\text{CH}_3)_2\text{Al}(\text{O}_2)\text{OH}_2$). This process forms a three-membered structure $(\text{CH}_3)_2\text{AlO}_2:\text{OH}_2$ (-0.9 kcal/mol) via TS_{1d} (5.1 kcal/mol). From $(\text{CH}_3)_2\text{AlO}_2:\text{OH}_2$ a release of water molecule occurs to form the product of $(\text{CH}_3)_2\text{AlO}_2$. The reaction energy for the final products ($(\text{CH}_3)_2\text{AlO}_2 + \text{CH}_3 + \text{H}_2\text{O}$) is exothermic by -13.0 kcal/mol relative to the reactants. The Al–O

bond length is 2.216 Å at the transition structure TS_{1d} and it is finally reduced to 1.890 Å in the three-membered ring $(\text{CH}_3)_2\text{AlO}_2$. The length of the O_2 double bond increases from 1.203 Å at the beginning to 1.348 Å when the reaction is completed (Fig. 3). The energy barrier is 19.4 kcal/mol at the CCSD(T) level which indicate that the generation of a reactive product such as radical CH_3 can occur under mild conditions.

4. Concluding remarks

In the present theoretical study, we have mapped out in detail the potential energy surfaces for the reactions of TMAI and O_2 and/or H_2O molecules. In particular, the possible reactions investigated include $\text{TMAI} + \text{O}_2 \rightarrow \text{CH}_3 + (\text{CH}_3)_2\text{AlO}_2$, $\text{TMAI} + \text{H}_2\text{O} \rightarrow \text{CH}_3 + \text{AlO} + 2\text{CH}_4$ and $\text{TMAI} + \text{H}_2\text{O} + \text{O}_2 \rightarrow \text{CH}_3 + (\text{CH}_3)_2\text{Al}(\text{O}_2)\text{OH}_2 \rightarrow \text{CH}_3 + (\text{CH}_3)_2\text{AlO}_2 + \text{H}_2\text{O}$. In the reaction of TMA with O_2 , a stable intermediate could not be directly formed. Instead, it takes place directly via a transition state lying 16.9 kcal/mol above the reactants, producing the $(\text{CH}_3)_2\text{AlO}_2$ intermediate, in which one of the methyls is slightly pushed away from Al. This methyl could be readily released from the Al to give CH_3 with a small amount of activation energy.

In the reaction of TMA with H_2O , TMA bonds with the water molecule forming a complex, $(\text{CH}_3)_3\text{AlOH}_2$, with 15.1 kcal/mol energy released. One methane molecule could be released from an intermediate, $(\text{CH}_3)_2\text{AlOH}$ with a 15.1 kcal/mol barrier. It is possible to deliver another methane molecule but it has to overcome a much higher barrier of 29.8 kcal/mol. Thus the overall mechanism contains four steps. The first two reactions are exothermic and can occur readily, whereas the last two processes are endothermic. The barrier for the formation of CH_3AlO is 29.8 kcal/mol, which cannot be easily overcome in the atmosphere.

In the termolecular reaction, $\text{TMA} + \text{O}_2 + \text{H}_2\text{O}$, the interaction of O_2 with TMA– H_2O complex gives a triplet $(\text{CH}_3)_3\text{AlOH}_2:\text{O}_2$ complex lying 16.9 kcal/mol below the reactants; the intermediate can fragment with a 35.1 kcal/mol barrier (about two times that of TS_{1a} barrier) to give CH_3 and $(\text{CH}_3)_2\text{Al}(\text{O}_2)\text{OH}_2$; the latter water complex can readily rearrange and fragment to produce $(\text{CH}_3)_2\text{AlO}_2 + \text{H}_2\text{O}$. The high barrier for the production of the CH_3 radical from the first water complex clearly reflects the retarding effect of H_2O on the production of the first CH_3 radical.

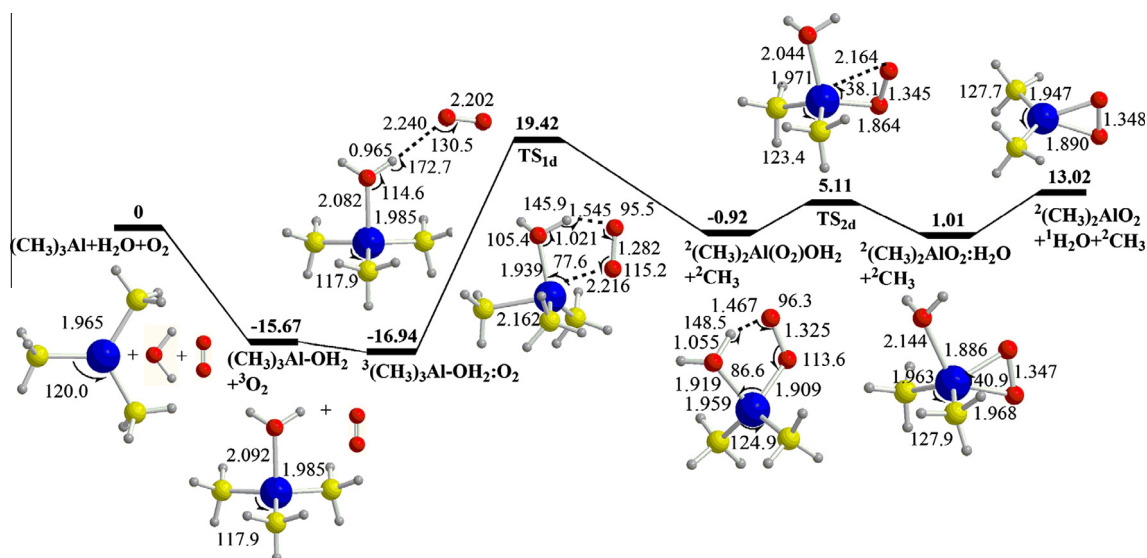


Fig. 3. Potential energy profile showing the $(\text{CH}_3)_3\text{Al} + \text{H}_2\text{O} + \text{O}_2$ reaction. Relative energies (kcal/mol) are calculated using the CCSD(T)/6-311+G(d,p)//B3LYP/6-311++G(3df,2p) + ZPE level. Selected bond lengths are given in angstrom and angles in degree.

These 3 processes apparently cannot generate CH_3 radicals easily to initiate the hypergolic reaction TMA in the air; they may contribute to the production of more reactive radicals in the flame region, once the combustion process is initiated. Our remaining task is to identify which reaction(s) involving TMA can take place with low energy barriers and be responsible for the hypergolic ignition process. Calculations are underway, for example, on reactions involving stable TMA dimer with O_2 , without and with the H_2O effect.

Acknowledgements

We are grateful for a partial support from the ATU Plan of MOE, Taiwan. M.C.L. acknowledges the support from the Taiwan Semiconductor Manufacturing Company for the TSMC Distinguished Professorship and for the National Science Council of Taiwan for the Distinguished Visiting Professorship at National Chiao Tung University in Hsinchu, Taiwan. Hue M.T. Nguyen thanks the National Foundation for Science and Technology Development (Nafosted) Vietnam, which has sponsored this work under the project number of 104.03.2010.29.

Appendix A. Supplementary material

Supplementary data associated with this article can be found, in the online version, at <http://dx.doi.org/10.1016/j.comptc.2014.02.015>.

References

- [1] A.R. Barron, MOCVD of group III chalcogenides, *Adv. Mater. Opt. Electron* 5 (1995) 245–285.
- [2] W.T. Kim, C.D. Kim, Optical energy gaps $\beta\text{-In}_2\text{S}_3$ thin films grown by spray pyrolysis, *J. Appl. Phys.* 60 (1986) 2631–2633.
- [3] N.M. Gasanly, A. Aydinli, Low-temperature photoluminescence spectra of InS single crystals, *Solid State Commun.* 101 (1997) 797–799.
- [4] T. Asikainen, M. Ritala, M. Leskela, Growth of In_2S_3 thin films by atomic layer epitaxy, *Appl. Surf. Sci.* 82 (83) (1994) 122–125.
- [5] (a) W. Rehwald, G. Harbeke, On the conduction mechanism in single crystal β -indium sulfide In_2S_3 , *J. Phys. Chem. Solids* 26 (1965) 1309–1318; (b) A.W. Ott, J.M. Johnson, J.W. Klaus, S.M. George, Surface chemistry of In_2O_3 deposition using $\text{In}(\text{CH}_3)_3$ and H_2O in a binary reaction sequence, *Appl. Surf. Sci.* 112 (1997) 205–215; (c) K. Ozasa, T. Ye, Y. Aoyagi, Deposition of thin indium oxide film and its application to selective epitaxy for in situ processing, *Thin Solid Films* 246 (1994) 58–64; (d) M.C. Rodriguez, A. Tiburcio-silver, A. Ortiz, A. Sanchezjuarez, Optoelectronic properties of indium sulfide thin films prepared by spray pyrolysis for photovoltaic applications, *Thin. Solid Films* 480 (2005) 133–137.
- [6] H. Kuramoto, H. Taniguchi, Transparent AlN ceramics, *J. Mater. Sci. Lett.* 3 (1984) 471–474.
- [7] L.V. Interrante, L.E. Carpenter II, C. Whitmarsh, W. Lee, M. Garbaskas, G.A. Slack, Studies of organometallic precursors to aluminum nitride, *Mater. Res. Soc. Symp. Proc.* 73 (1986) 359–366.
- [8] M.E. Bartram, T.A. Michalske, J.W. Rodgers Jr., T.M. Mayer, Chemisorption of trimethylaluminum and ammonia on silica: mechanisms for the formation of aluminum–nitrogen bonds and the elimination of methyl groups bonded to aluminum, *Chem. Mater.* 3 (1991) 953–960.
- [9] H.O. Pierson, *Handbook of Chemical Vapor Deposition*, Noyes Publications, Edgewood, NJ, 1992.
- [10] C. Soto, V. Boiadjev, W.T. Tysoe, Spectroscopic study of AlN film formation by the sequential reaction of ammonia and trimethylaluminum on alumina, *Chem. Mater.* 8 (1996) 2359–2365.
- [11] M. Juppo, A. Rahtu, M. Ritala, M. Leskela, In situ mass spectrometry study on surface reactions in atomic layer deposition of Al_2O_3 thin films from trimethylaluminum and water, *Langmuir* 16 (2000) 4034–4039.
- [12] T. Suntola, J. Antson, A. Pakkala, S. Lindfors, *Thin Film Electroluminescent device, SID 80 Digest*, vol. 11, 1980, pp. 108–109.
- [13] S. Strite, H. Morkoç, GaN, AlN, and InN: a review, *J. Vac. Sci. Technol. B* 10 (1992) 1237–1266.
- [14] H.U. Baier, W. Monch, Growth of AlN on GaAs(110) by reactive molecular beam deposition, *J. Vac. Sci. Technol. B* 10 (1992) 1735–1739.
- [15] R.R. Tummala, E.J. Rymaszewski, *Microelectronics Packaging Handbook*, Van Nostrand-Reinhold, New York, 1989.
- [16] R.P. O'Toole, S.G. Burns, G.J. Bastiaans, Thin aluminum nitride film resonators: miniaturized high sensitivity mass sensors, *Anal. Chem.* 64 (1992) 1289–1294.
- [17] A.C. Jones, S.A. Rushworth, D.J. Houlton, J.S. Roberts, V. Roberts, C.R. Whitehouse, G.W. Critchlow, Deposition of aluminum nitride thin films by MOCVD from the trimethylaluminum–ammonia adduct, *Chem. Depos.* 2 (1996) 5–8.
- [18] J.J. Eisch, in: E.W. Abel, F.G.A. Stone, G. Wilkinson (Eds.), *Comprehensive Organometallic Chemistry II: A Review of the Literature 1982–1994*, vol. 1, Pergamon, Oxford, UK, 1995, p. 431.
- [19] S.S. Reddy, S. Sivaram, Homogeneous metallocene–methylaluminoxane catalyst systems for ethylene polymerization, *Prog. Polym. Sci.* 20 (1995) 309–367.
- [20] H. Sinn, W. Kaminsky, H.J. Vollmer, R. Woldt, “Living Polymers” on polymerization with extremely productive ziegler catalysts, *Angew. Chem. Int. Ed. Engl.* 19 (1980) 390–392.
- [21] M.R. Mason, J.M. Smith, S.G. Bott, A.R. Barron, Hydrolysis of tri-tert-butylaluminum: the first structural characterization of alkylalumoxanes, $[(\text{R}_2\text{Al})_2\text{O}]_n$ and $(\text{RAIO})_n$, *J. Am. Chem. Soc.* 115 (1993) 4971–4984.
- [22] M.J. Frisch et al., *Gaussian Inc*, Pittsburgh PA, 2003.
- [23] Y. Widjaja, C.B. Musgrave, Quantum chemical study of the mechanism of aluminum oxide atomic layer deposition, *Appl. Phys. Lett.* 80 (2002) 3304–3306.
- [24] M.K. Ghosh, C.H. Choi, The initial mechanisms of Al_2O_3 atomic layer deposition on $\text{OH}/\text{Si}(100) - 2 \times 1$ surface by tri-methylaluminum and water, *Chem. Phys. Lett.* 426 (2006) 365–369.